UAV-Aided Secure Short-Packet Data Collection and Transmission

Xinying Chen, Nan Zhao, *Senior Member, IEEE*, Zheng Chang, *Senior Member, IEEE*, Timo Hämäläinen, *Senior Member, IEEE*, and Xianbin Wang, *Fellow, IEEE*

***Abstract*— Benefiting from the deployment flexibility and the line-of-sight (LoS) channel conditions, unmanned aerial vehicle (UAV) has gained tremendous attention in data collection for wireless sensor networks. However, the high-quality air-ground channels also pose significant threats to the security of UAV-aided wireless networks. In this paper, we propose a short-packet secure UAV-aided data collection and transmission scheme to guarantee the freshness and security of the transmission from the sensors to the remote ground base station (BS). First, during the data collection phase, the trajectory, the flight duration, and the user scheduling are jointly optimized with the objective of maximizing the energy efficiency (EE). To solve the non-convex EE maximization problem, we adopt the first-order Taylor expansion to convert it into two convex subproblems, which are then solved via successive convex approximation. Furthermore, we consider the maximum rate of transmission in the UAV data transmission phase to achieve a maximum secrecy rate. The transmit power and the blocklength of UAV-to-BS transmission are jointly optimized subject to the constraints of eavesdropping rate and outage probability. Simulation results are provided to validate the effectiveness of the proposed scheme.**

***Index Terms*— Data collection, finite blocklength, resource allocation, secure transmission, short-packet transmission, unmanned aerial vehicle.**

I. Introduction

CONSIDERED as a flexible network entity in the beyond fifth generation and the sixth generation (B5G/6G) mobile communications [2], [3], the unmanned aerial vehicle (UAV) aided networks have recently attracted significant attention. The benefits of high mobility, low cost, easy deployment, and line-of-sight (LoS) links allow UAVs to be utilized in different scenarios to improve the wireless network performance [4], [5]. With these advantages, UAVs can be deployed as high-mobility users, fast-configured base stations (BSs), or long-range relays [6]. Specifically, the flexibility of UAV enables efficient data collection for B5G/6G Internet of things (IoTs) [7], [8], [9], which can tackle the challenge of collecting data from remote or extreme environments. Instead of exhaustively collecting data from each user randomly, the energy efficiency (EE) of UAV can be improved via the proper design of trajectory and user scheduling [10], [11], [12]. Wang et al. proposed an efficient data collecting scheme for a non-orthogonal multiple access (NOMA) UAV network to minimize the flight duration in [10] via jointly designing the trajectory, scheduling, and transmit power. To keep the data freshness of wireless sensor networks, Liu et al. proposed an efficient data collection scheme in [11] to minimize the age of information of all the sensors via properly designing the trajectory of UAV collector. In [12], an energy harvesting wireless sensor scheme was studied by Liu et al., where the UAV transfers energy to support the sensor nodes and minimizes the outage probability of data collection.

However, information security threat resulting from the LoS channels cannot be ignored during the UAV data collection process [13], [14], [15], [16]. In [13], Zhang et al. proposed two secure schemes to enable the information security via cooperative dual UAVs with the energy limit of UAV considered. To preserve the privacy of devices, Yang et al. proposed a federal learning based scheme for UAV-assisted networks in [14] to provide reliable and efficient data collection. In [15], Xu et al. utilized blockchain in a UAV-assisted data collection IoT network to guarantee the information security and improve the EE. In [16], Xu et al. investigated the secure transmission in a dual UAV mobile edge computing system under both time division multiple access and NOMA. To tackle the security challenges, many studies have been focused on improving the security in UAV-related systems [17], [18], [19], [20]. In [17], Chen et al. proposed a resource allocation scheme to realize the secure transmission in circular-trajectory UAV-NOMA networks. Wang et al. introduced the simultaneous wireless information and power transfer into NOMA-UAV networks in [18] to provide secure transmission while guaranteeing the energy supplement for passive receivers. In [19], Zhong et al.

Manuscript received 14 May 2022; revised 13 November 2022; accepted 5 February 2023. Date of publication 14 February 2023; date of current version 18 April 2023. The work of Nan Zhao is supported in part by the National Natural Science Foundation of China (NSFC) under Grant 62271099 and 62071105. An earlier version of this paper was presented in part at the IEEE GLOBECOM 2022 [DOI: 10.1109/GLOBECOM48099.2022.10000768]. The associate editor coordinating the review of this article and approving it for publication was J. Liu. *(Corresponding author: Zheng Chang.)*

Xinying Chen is with the Faculty of Information Technology, University of Jyväskylä, 40014 Jyväskylä, Finland, and also with the School of Information and Communication Engineering, Dalian University of Technology, Dalian 116024, China (e-mail: cxy@mail.dlut.edu.cn).

Nan Zhao is with the School of Information and Communication Engineering, Dalian University of Technology, Dalian 116024, China (e-mail: zhaonan@dlut.edu.cn).

Zheng Chang is with the School of Computer Science and Engineering, University of Electronic Science and Technology of China, Chengdu 610051, China, and also with the Faculty of Information Technology, University of Jyväskylä, 40014 Jyväskylä, Finland (e-mail: zheng.chang@jyu.fi).

Timo Hämäläinen is with the Faculty of Information Technology, University of Jyväskylä, 40014 Jyväskylä, Finland (e-mail: timo.t.hamalainen@jyu.fi).

Xianbin Wang is with the Department of Electrical and Computer Engineering, Western University, London, ON N6A 5B9, Canada (e-mail: xianbin.wang@uwo.ca).

Color versions of one or more figures in this article are available at https://doi.org/10.1109/TCOMM.2023.3244954.

Digital Object Identifier 10.1109/TCOMM.2023.3244954

leveraged the power and trajectory control over both the UAV transmitter and a friendly UAV jammer to avoid being eavesdropped. Kang et al. integrated the blockchain into UAV communications in [20] to share data securely.

In addition, because of the short packets used in the UAV data collection, the conventional performance analysis based on infinite blocklength cannot characterize the system accurately [21], [22]. This motivates new research to investigate the performance of short-packet transmission, which mainly focuses on improving the reliability and reducing the time delay [23], [24]. When evaluating the performance in typical wireless communications, the infinite blocklength (or sufficient large blocklength) is commonly considered, where the critical performance parameter can be accurately modeled. However, data transmission in IoT applications usually consists of a large amount of time-intolerant and error-intolerant information, where the length of message is short. Thus, applying short packets to UAV-related communications could make the information transmission more effective [25], [26], [27]. In [25], Ranjha and Kaddoum utilized the UAV and reconfigurable intelligent surface to achieve a short-packet IoTs system aiming to minimize the decoding error rate. Ren et al. studied the short-packet communication in UAV-assisted networks [26], where the achievable finite blocklength data rate is investigated under three-dimension channel models. In [27], the blocklength and hovering location of UAV relay were optimized by Pan et al. to minimize the decoding error probability at the receiver.

As observed, using finite blocklength to explore the physical layer security of UAV-aided networks is still under investigation, and the security for IoT networks is also of critical importance. The finite-blocklength security for UAV-assisted data collection and transmission has not been well studied in the aforementioned literature. Thus, in this paper, we propose a short-packet secure UAV data collection scheme to guarantee the information secrecy and freshness. We summarize the main contribution of this paper as follows.

- To our best knowledge, this is the first work considering the secure transmission of short packets for UAV-assisted data collection. Specifically, user scheduling, flight duration, and trajectory are jointly designed to achieve higher EE in the data collection via UAV. Then, in the data transmission to BS, the finite blocklength and transmit power of UAV are jointly optimized to maximize the secrecy rate while restricting the eavesdropping rate and the secrecy outage probability.
- During the first phase of data collection, the trajectory and user scheduling problem is formulated as non-convex, which cannot be solved directly. Thus, we utilize the successive convex approximation (SCA) and first-order Taylor expansion to transfer the non-convex problem into two convex subproblems and solve them iteratively to derive the optimal solution for higher EE.
- We jointly analyze the monotonicity of the lower bound of secrecy rate, the eavesdropping rate and the outage probability to derive the optimal transmit power and the optimal blocklength for the second secure short-packet transmission phase. Without awareness of the channel state information of the eavesdropper, we perform statistical analysis on the eavesdropping rate to derive the optimal solution for the secure transmission.

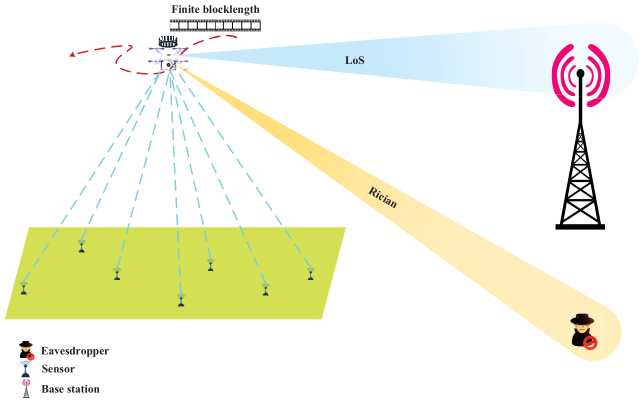

Fig. 1. UAV-assisted short-packet data collection and secure transmission.

The rest of this paper is organized as follows. In Section II, we describe the system model. The EE maximization problem is formulated and optimized in Section III. Then, the secrecy rate maximization for short-packet secure transmission is given and solved in Section IV. We present the simulation results in Section V, and conclude the work in Section VI.

Notation: Boldface lowercase and uppercase letters identify vectors and matrices, respectively. $\mathbb{C}^{M\times N}$ represents the $M \times N$ complex matrix. $\mathbf{a}^H$ and $\|\mathbf{a}\|$ are the conjugate transpose and Euclidean norm of vector $\mathbf{a}$, respectively. $Pr\{x\}$ and $E[x]$ are the probability and the expectation of the random variable x. $\mathcal{CN}(\mu, \sigma^2)$ denotes the complex Gaussian distribution with mean μ and variance σ^2. $I_0(*)$ represents the first-kind and the zero-order Bessel function. $\chi^2(k, \lambda)$ represents the non-central chi-square distribution with k degrees of freedom and the non-centrality parameter of λ.

II. System Model

In the network, a UAV collects data from randomly distributed sensors, and then transmits them to the BS, as shown in Fig. 1. The data transmission consists of two parts, namely the data collection phase and the secure transmission phase. The sensors, the BS, and the eavesdropper are all assumed to equip with a single antenna. The UAV is assumed to have a single receiving antenna and multiple transmitting antennas. In the data collection phase, the UAV flies according to its designed trajectory $\mathbf{w}$ and collects data from the sensors according to their scheduling variable $t_i[n]$. After data collection, the UAV transmits the received data via precoding to the legitimate BS while avoiding being eavesdropped by the eavesdropper. The distributed area of sensors is assumed to be much smaller compared with the distance between the UAV and BS, which leads to a tiny impact of the UAV trajectory on the transmission performance towards the BS in the second phase. Therefore, in the proposed scheme, we first design the trajectory of UAV, and then characterize the secure transmission to the BS, which is described as follows.

A. Data Collection Phase

There are S sensors randomly distributed in the square area with the length of each side as L, where the location of the i-th sensor can be expressed as $L_i(x_i, y_i, 0) \in R^{1\times 3}$, $\forall i \in \{1, \cdots, S\}$. During the data collection, the UAV flies over the area with a fixed height H. The data collection phase is conducted for a duration T, which is equally divided into N slots. Therefore, the duration of each time slot can be expressed as $\Delta t = \frac{T}{N}$. Then, the trajectory of UAV can be simplified as $\mathbf{w} = [w[1], \cdots, w[n], \cdots, w[N]]$, where $w[n] = (x[n], y[n], H) \in R^{1\times 3}, \forall n = \{1, \cdots, N\}$ is the location of UAV in the n-th slot. Besides, the UAV can adjust its trajectory $\mathbf{w}$ and speed $v \leq V_{max}$ to achieve better transmission performance, where V_{max} is the maximum achievable speed of UAV. Assume that the UAV returns to its original location after finishing the data collection within T, and we have

$$w[1] = w[N]. \tag{1}$$

In addition, the duration of each slot is small. Thus, $\Delta_{uav}[n] = ||w[n] - w[n-1]||$ can be approximately unchanged compared to H, which is expressed as

$$\Delta_{uav}[n] \leq \Delta t V_{max}, \quad n = 2, \cdots, N, \tag{2}$$

and

$$\Delta_{uav}[n] \leq \theta H, \quad n = 2, \cdots, N, \tag{3}$$

where $0 < \theta \ll 1$.

In the data collection, the i-th sensor should transmit at least B_i bits to the UAV during its assigned time slots. Consider that the UAV adopts time-division multiple access, which indicates that the UAV only serves one user within each time slot. Define a boolean symbol $t_i[n]$, $\forall i \in \{1, \cdots, S\}$ and $\forall n \in \{1, \cdots, N\}$, to describe the scheduling variable for all sensors, where $t_i[n] = 1$ represents that the i-th sensor can send data to the UAV during the n-th slot and $t_i[n] = 0$ indicates that the i-th sensor keeps silence. The scheduling variable $t_i[n]$ can be described as

$$t_i[n] = \{0, 1\}, \quad \forall i \in \{1, \cdots, S\}, \quad \forall n \in \{1, \cdots, N\}, \tag{4}$$

and

$$\sum_{i=1}^{S} t_i[n] \leq 1, \quad \forall n \in \{1, \cdots, N\}. \tag{5}$$

Assume that the channel coefficient $g_{s_i u}$ between the i-th sensor and UAV follows the large-scale LoS channel, which can be described as

$$g_{s_i u} = \sqrt{\frac{\rho_0}{d_{s_i u}^{\alpha}}}, \quad \forall i \in \{1, \cdots, S\}, \tag{6}$$

where ρ_0 is the path loss reference at 1 m for LoS, and α represents the path loss exponent. $d_{s_i u}$ denotes the distance between the i-th sensor and UAV, which can be denoted as

$$d_{s_i u} = ||L_i - w[n]||, \quad \forall i \in \{1, \cdots, S\}. \tag{7}$$

The blocklength of each sensor is assumed to be N_s. Apart from the traditional data rate in an infinite system, the capacity should take the decoding error probability ϵ_s at the UAV into consideration. Thus, the transmission rate of the i-th sensor during the n-th slot can be described as

$$R_i[n] = t_i[n] \log_2 \left[(1 + \gamma_i[n]) - \sqrt{\frac{V_i[n]}{N_s}} \frac{Q^{-1}(\epsilon_s)}{\ln 2} \right], \tag{8}$$

where $Q^{-1}(*)$ represents the inverse Q-function. The signal-to-noise ratio (SNR) $\gamma_i[n]$ can be described as

$$\gamma_i[n] = \frac{P_s \rho_0}{d_{s_i u}^{\alpha} \sigma^2}, \tag{9}$$

where σ^2 represents the variance of the Gaussian noise and P_s is the transmit power of each sensor. In addition, $V_i[n]$ in (8) can be defined as

$$V_i[n] = 1 - (1 + \gamma_i[n])^{-2}. \tag{10}$$

Thus, the total transmitted data D_{sen} from the distributed sensors within the whole duration T can be defined as

$$D_{sen} = \sum_{i=1}^{S} \sum_{n=1}^{N} R_i[n] \Delta t. \tag{11}$$

The UAV is assumed to be rotary-wing, and its propulsion power is much higher than the communication part. Thus, we only consider the propulsion energy in the trajectory design when maximizing the EE. The power consumed by the UAV during the n-th time slot to support flying can be described as (12), shown at the bottom of the next page, where its parameters can be referred to Table I.

TABLE I
PARAMETER DEFINITIONS IN (12)

Parameter	Definition
P_{bld}	Profile power of blades
v_t	Tip speed of rotor blades
r_{drag}	Fuselage drag ratio
ρ_{air}	Density of air
h_{rtor}	Solidity of rotor
S_{rtor}	Disc area of rotor
P_{ind}	Induced power when $\frac{\Delta uav[n]}{\Delta t} = 0$
$\bar{v}$	Mean induced speed of motor

Based on (12), the total propulsion energy consumption E_{uav} of UAV can be calculated as

$$E_{uav} = \sum_{n=1}^{N} P_{uav}[n] \Delta t. \tag{13}$$

Then, the EE r_{tc} can be defined as

$$r_{tc} = \frac{D_{sen}}{E_{uav}}. \tag{14}$$

We also constrain the consumed energy of the i-th sensor to be smaller than its total energy E_i as

$$\sum_{n=1}^{N} t_i[n] P_s \Delta t \leq E_i, \tag{15}$$

and the transmitted data of the i-th sensor to be no smaller than its sensed data B_i as

$$\sum_{n=1}^{N} R_i[n]\Delta t \geq B_i. \tag{16}$$

B. Secure Short-Packet Transmission Phase

After receiving the data from the sensors, the UAV transmits them to the BS with M antennas in blocklength N_u, where the BS locates at $L_b(x_b, y_b, z_b) \in R^{1\times 3}$. Assume that the channel coefficient $\mathbf{g}_b[n]$ in the n-th time slot between the UAV and BS follows the large-scale LoS path loss, which can be expressed as

$$\mathbf{g}_b[n] = \sqrt{\frac{\rho_0}{d_b[n]^\alpha}}\mathbf{h}_b[n], \tag{17}$$

where $d_b[n] \triangleq ||L_b - w[n]||, \forall n \in \{1, \cdots, N\}$, is the distance between the UAV and BS at the n-th slot, and $\mathbf{h}_b[n] \triangleq \{h_{b_1}[n], \cdots, h_{b_M}[n]\} \in \mathbb{C}^{1\times M}$ represents the LoS channel components between the M antennas of UAV and the BS, where $\forall |h_{b_i}[n]| = 1$ for $i \in \{1, \cdots, M\}$ is the channel coefficient for the i-th antenna.

In addition, there exists a terrestrial eavesdropper located near the BS, and the UAV does not know its accurate location. Thus, we analyze the secure transmission under the worst situation, where the closest location of the eavesdropper to the UAV is estimated at $L_e(x_e, y_e, 0) \in R^{1\times 3}$. Assume that the channel coefficient $\mathbf{g}_e[n]$ during each time slot between the UAV and eavesdropper follows a large-scale path loss and a small-scale Rician fading as

$$\mathbf{g}_e[n] = \sqrt{\frac{\rho_0}{d_e[n]^\alpha}}\left(c_L\mathbf{h}_{eL}[n] + c_N\mathbf{h}_{eN}[n]\right) = \sqrt{\frac{\rho_0}{d_e[n]^\alpha}}\mathbf{h}_e[n], \tag{18}$$

which cannot be obtained by the UAV. $d_e[n] \triangleq ||L_e - w[n]||, \forall n \in \{1, \cdots, N\}$, is the distance between the UAV and eavesdropper during the n-th time slot. $c_L = \sqrt{\frac{K}{1+K}}$ and $c_N = \sqrt{\frac{1}{1+K}}$ are the LoS and non-LoS (NLoS) channel coefficients of Rician fading, where K is the Rician factor. The LoS channel component $\mathbf{h}_{eL}[n] \triangleq \{h_{eL_1}[n], \cdots, h_{eL_M}[n]\} \in \mathbb{C}^{1\times M}$ follows $|h_{eL_i}[n]| = 1, \forall i \in \{1, \cdots, M\}$, and the Rayleigh fading component $\mathbf{h}_{eN}[n] \triangleq \{h_{eN_1}[n], \cdots, h_{eN_M}[n]\} \in \mathbb{C}^{1\times M}$ satisfies $h_{eN_i}[n] \sim \mathcal{CN}(0, 1), \forall i \in \{1, \cdots, M\}$.

Assume that the UAV performs the maximum ratio transmission (MRT) via precoding towards the BS, where the precoding vector $\mathbf{u}[n]$ during each slot at the UAV can be described as

$$\mathbf{u}[n] = \frac{\mathbf{h}_b^H[n]}{||\mathbf{h}_b[n]||}. \tag{19}$$

The UAV precodes the transmitted signal of blocklength N_u with transmit power P_a, where the received SNR at the BS during the n-th slot can be described as

$$\gamma_b[n] = \frac{P_a\rho_0|\mathbf{h}_b[n]\mathbf{u}[n]|^2}{\sigma^2 d_b[n]^\alpha} = \frac{P_a\rho_0 M}{\sigma^2 d_b[n]^\alpha}. \tag{20}$$

Similar to the SNR at the BS, the SNR at the malicious eavesdropper can be described as

$$\gamma_e[n] = \frac{P_a\rho_0|\mathbf{h}_e[n]\mathbf{u}[n]|^2}{\sigma^2 d_e[n]^\alpha}. \tag{21}$$

Similar to (8), the channel capacities from the UAV to both the BS and eavesdropper are smaller than the traditional infinite blocklength transmission. The maximum achievable transmission rate $R_b[n]$ of each slot can be expressed as

$$R_b[n] = \log_2(1 + \gamma_b[n]) - \sqrt{\frac{\gamma_b[n](\gamma_b[n]+2)}{N_u(\gamma_b[n]+1)^2}}\frac{Q^{-1}(\epsilon)}{\ln 2}, \tag{22}$$

where $n \in \{1, \cdots, N\}$. ϵ is the maximum allowed error decoding probability. The maximum achievable eavesdropping rate at the eavesdropper can be demonstrated as

$$R_e[n] = \log_2(1 + \gamma_e[n]) - \sqrt{\frac{\gamma_e[n](\gamma_e[n]+2)}{N_u(\gamma_e[n]+1)^2}}\frac{Q^{-1}(\delta_e)}{\ln 2}, \tag{23}$$

where $n \in \{1, \cdots, N\}$, and δ_e is the information leakage probability.

Based on [28], the lower bound to the secrecy rate $R_s[n]$ during each time slot can be described as (24), shown at the bottom of the next page.

The secure transmission outage occurs when the transmission rate $R_0[n]$ of the n-th slot is larger than the secrecy rate capacity. To guarantee the security, we define the secrecy outage probability $p_{out}[n]$ in each time slot as

$$p_{out}[n] = Pr\left\{R_s[n] \leq R_0[n]\right\}, \tag{25}$$

In the following, the EE maximization for data collection is investigated in Section III, while the secrecy rate in short-packet transmission is maximized in Section IV.

III. Energy Efficiency Maximization

Owning to the energy limitation, the maximum flying duration of UAV is limited. To balance between the flight duration of UAV and the amount of collected data, we optimize the trajectory of UAV and the scheduling variable of each sensor to achieve higher EE for data collection in this section.

$$P_{uav}[n] = P_{bld}\left(1 + \frac{3\Delta_{uav}[n]^2}{v_t^2\Delta t^2}\right) + \frac{1}{2}r_{drag}\rho_{air}h_{rtor}S_{rtor}\frac{\Delta_{uav}[n]^3}{\Delta t^3} + P_{ind}\left(\sqrt{1 + \frac{\Delta_{uav}[n]^4}{4\bar{v}^4\Delta t^4}} - \frac{\Delta_{uav}[n]^2}{2\bar{v}^2\Delta t^2}\right)^{\frac{1}{2}}. \tag{12}$$

A. Problem Formulation

The trajectory $\mathbf{w}$ of UAV and the scheduling vector $\mathbf{t} \triangleq \{t_i[n], \forall i = \{1, \cdots, S\}, \forall n = \{1, \cdots, N\}\}$ are optimized. In addition, we also optimize the total flight duration of UAV to achieve a higher EE. By optimizing the trajectory $\mathbf{w}$ of UAV, the scheduling vector $\mathbf{t}$, and the flight duration T, we aim at maximizing EE r_{tc}. The optimization problem can be formulated as

$$\mathbf{P1:} \quad \max_{\mathbf{w},\mathbf{t},T} \ r_{tc} \tag{26a}$$
$$s.t. \ w[1] = w[N], \tag{26b}$$
$$\Delta_{uav}[n] \le \Delta t V_{max}, \tag{26c}$$
$$\Delta_{uav}[n] \le \theta H, \tag{26d}$$
$$\sum_{n=1}^{N} t_i[n] P_s \Delta t \le E_i, \tag{26e}$$
$$\sum_{n=1}^{N} R_i[n] \Delta t \ge B_i, \tag{26f}$$
$$\sum_{i=1}^{S} t_i[n] \le 1, \tag{26g}$$
$$0 \le t_i[n] \le 1, \tag{26h}$$

which has a non-convex structure and is difficult to solve. Thus, we propose an iterative algorithm to solve the proposed problem via SCA. We first optimize the scheduling vector $\mathbf{t}$ and flight duration T with a given trajectory $\mathbf{w}$. Then, with the optimized $\mathbf{t}$ and T, the trajectory $\mathbf{w}$ can be updated.

B. Optimization of Scheduling and Flight Duration

According to the definition of Δt, we reformulate P1 as the optimization of Δt instead of T, since r_{tc} is the expression of Δt. Thus, for a given trajectory $\mathbf{w}$ of UAV, the problem P1 can be simplified as

$$\mathbf{P1.1:} \quad \max_{\mathbf{t},\Delta t} \ \frac{\sum_{i=1}^{S}\sum_{n=1}^{N} R_i[n]\Delta t}{E_{ucvx}(\Delta t) + E_{uNcvx}(\Delta t)} \tag{27a}$$
$$s.t. \ \Delta_{uav}[n] \le \Delta t V_{max}, \tag{27b}$$
$$\sum_{n=1}^{N} t_i[n] P_s \Delta t \le E_i, \tag{27c}$$
$$\sum_{n=1}^{N} R_i[n] \Delta t \ge B_i, \tag{27d}$$
$$\sum_{i=1}^{S} t_i[n] \le 1, \tag{27e}$$
$$0 \le t_i[n] \le 1, \tag{27f}$$

where $E_{uav} = E_{ucvx}(\Delta t) + E_{uNcvx}(\Delta t)$. $E_{ucvx}(\Delta t)$ is the convex component in E_{uav} with respect to Δt, and can be described as

$$E_{ucvx}(\Delta t) = \sum_{n=1}^{N} P_{bld}\left(\Delta t + \frac{3\Delta_{uav}[n]^2}{v_t^2 \Delta t}\right) + \frac{1}{2} r_{drag}\rho_{air} h_{rtor} S_{rtor} \sum_{n=1}^{N} \frac{\Delta_{uav}[n]^3}{\Delta t^2}. \tag{28}$$

$E_{uNcvx}(\Delta t)$ is the non-convex component in E_{uav} with respect to Δt, and can be described as

$$E_{uNcvx}(\Delta t) = P_{ind} \sum_{n=1}^{N} \left(\sqrt{\Delta t^4 + \frac{\Delta_{uav}[n]^4}{4\bar{v}^4}} - \frac{\Delta_{uav}[n]^2}{2\bar{v}^2}\right)^{\frac{1}{2}}. \tag{29}$$

From (27), we can see that $\sum_{i=1}^{S}\sum_{n=1}^{N} R_i[n]\Delta t$ is non-concave and $E_{uNcvx}(\Delta t)$ is non-convex, which makes P1.1 mathematically unsolvable. Therefore, we introduce an auxiliary parameter $R_N[i]$ as

$$R_N[i]^2 = \sum_{n=1}^{N} R_i[n]\Delta t, \tag{30}$$

to transfer the non-concave (27a) into a different version, the numerator part of which can be changed into

$$D_{sen} = \sum_{i=1}^{S} R_N[i]^2. \tag{31}$$

In addition, we introduce another auxiliary parameter $z[n]$ to upper bound a complex component in E_{uNcvx} as

$$z[n]^2 \ge \sqrt{\Delta t^4 + \frac{\Delta_{uav}[n]^4}{4\bar{v}^4}} - \frac{\Delta_{uav}^2}{2\bar{v}^2}. \tag{32}$$

By performing the simple algebra transformation on (32), we have

$$\Delta t^4 \le z[n]^4 + \frac{\Delta_{uav}[n]^2}{\bar{v}^2} z[n]^2, \tag{33}$$

which changes $E_{uNcvx}(\Delta t)$ in (29) into

$$E_{uNcvx}(\Delta t) \le P_{ind} \sum_{n=1}^{N} z[n]. \tag{34}$$

Then, P1.1 can be transformed as

$$\mathbf{P1.1.a:} \quad \max_{\mathbf{t},\Delta t, R_N[i], z[n]} \ \frac{\sum_{i=1}^{S} R_N[i]^2}{E_{ucvx}(\Delta t) + P_{ind}\sum_{n=1}^{N} z[n]} \tag{35a}$$
$$s.t. \ (27b), (27e), (27f), \tag{35b}$$
$$\sum_{n=1}^{N} t_i[n] P_s \le \frac{E_i}{\Delta t}, \tag{35c}$$
$$R_N[i]^2 \ge B_i, \tag{35d}$$

$$R_s[n] = \log_2(1+\gamma_b[n]) - \log_2(1+\gamma_e[n]) - \sqrt{\frac{\gamma_b[n](\gamma_b[n]+2)}{(\gamma_b[n]+1)^2}} \frac{Q^{-1}(\epsilon)}{\ln 2\sqrt{N_u}} - \sqrt{\frac{\gamma_e[n](\gamma_e[n]+2)}{(\gamma_e[n]+1)^2}} \frac{Q^{-1}(\delta_e)}{\ln 2\sqrt{N_u}}. \tag{24}$$

$$R_N[i]^2 \le \sum_{n=1}^{N} R_i[n]\Delta t, \tag{35e}$$

$$\Delta t^4 \le z[n]^4 + \frac{\Delta_{uav}[n]^2}{\bar{v}^2} z[n]^2. \tag{35f}$$

To ensure that (35) is mathematically solvable, we need to change (35c) and (35e) into concave ones with respect to Δt. Also, (35d) and (35f) need to be changed into concave ones with respect to $R_N[i]$ and $z[n]$, respectively.

We apply the first-order Taylor expansion to change the above-mentioned functions into their concave versions. Then, iteratively performing SCA, the optimal values of $\mathbf{t}$, Δt, $R_N[i]$, $z[n]$ can be achieved.

The first-order Taylor expansion of (35c) with a given point $\Delta t^{(r)}$can be expressed as

$$\frac{E_i}{\Delta t} \ge E_i \left(\frac{1}{\Delta t^{(r)}} - \left(\frac{1}{\Delta t^{(r)}} \right)^2 \left(\Delta t - \Delta t^{(r)} \right) \right) \ge \sum_{n=1}^{N} t_i[n] P_s, \tag{36}$$

where $\Delta t^{(r)}$ is assumed to be the optimal value of Δt in (35) from the r-th iteration.

Similarly, (35d) can be expanded at a given point $R_N^{(r)}[i]$ as

$$R_N[i]^2 \ge R_N^{(r)}[i]^2 + 2R_N^{(r)}[i] \left(R_N[i] - R_N^{(r)}[i] \right) \ge B_i, \tag{37}$$

where $R_N^{(r)}[i]$ is assumed to be the optimal value of $R_N[i]$ in (35) from the r-th iteration.

Also, according to the hyperbolic constraint [29], we have (35e) if and only if

$$\left\| \begin{bmatrix} 2R_N[i]^2 \\ \sum_{n=1}^{N} (R_i[n] - \Delta t) \end{bmatrix} \right\| \le \sum_{n=1}^{N} (R_i[n] - \Delta t). \tag{38}$$

We can replace (35e) with (38). The expansion of (35f) at a given point $z^{(r)}[n]$ can be changed to

$$\begin{aligned} &z[n]^4 + \frac{\Delta_{uav}[n]^2}{\bar{v}^2} z[n]^2 \\ &\ge z^{(r)}[n]^4 + 4z^{(r)}[n]^3 \left(z[n] - z^{(r)}[n] \right) \\ &\quad + \frac{\Delta_{uav}[n]^2}{\bar{v}^2} \left[z^{(r)}[n]^2 + 2\, z^{(r)}[n] \left(z[n] - z^{(r)}[n] \right) \right] \ge \Delta t^4, \end{aligned} \tag{39}$$

where $z^{(r)}[n]$ is assumed to be the optimal value of $z[n]$ in (35) from the r-th iteration.

Thus, P1.1.a can be changed into a mathematically solvable problem as

$$\textbf{P1.1.b:} \quad \max_{\mathbf{t}, \Delta t, R_N[i], z[n]} \frac{R_N^{(r)}[i]^2 + 2R_N^{(r)}[i] \left(R_N[i] - R_N^{(r)}[i] \right)}{E_{ucvx}(\Delta t) + P_{ind} \sum_{n=1}^{N} z[n]} \tag{40a}$$

$$s.t.\ (27b), (27e), (27f), \tag{40b}$$

$$E_i \left(\frac{1}{\Delta t^{(r)}} - \left(\frac{1}{\Delta t^{(r)}} \right)^2 \left(\Delta t - \Delta t^{(r)} \right) \right) \ge \sum_{n=1}^{N} t_i[n] P_s, \tag{40c}$$

$$R_N^{(r)}[i]^2 + 2R_N^{(r)}[i] \left(R_N[i] - R_N^{(r)}[i] \right) \ge B_i, \tag{40d}$$

$$R_N[i]^2 \le \sum_{n=1}^{N} R_i[n]\Delta t, \tag{40e}$$

$$\frac{\Delta_{uav}[n]^2}{\bar{v}^2} \left[z^{(r)}[n]^2 + 2\, z^{(r)}[n] \left(z[n] - z^{(r)}[n] \right) \right] \tag{40f}$$

$$z^{(r)}[n]^4 + 4z^{(r)}[n]^3 \left(z[n] - z^{(r)}[n] \right) \ge \Delta t^4,$$

$$\left\| \begin{bmatrix} 2R_N[i]^2 \\ \sum_{n=1}^{N} (R_i[n] - \Delta t) \end{bmatrix} \right\| \le \sum_{n=1}^{N} (R_i[n] - \Delta t), \tag{40g}$$

which is convex, and can be solved by existing convex programming tools such as CVX.

C. Optimization of UAV Trajectory

Then, we optimize the trajectory $\mathbf{w}$ of UAV with the given scheduling vector $\mathbf{t}$ and flight duration T. The optimization problem can be reformulated as

$$\textbf{P1.2:} \quad \max_{\mathbf{w}} \frac{\sum_{i=1}^{S} \sum_{n=1}^{N} R_i[n]\Delta t}{E_{ucvx}(\Delta t) + E_{uNcvx}(\Delta t)} \tag{41a}$$

$$s.t.\ w[1] = w[N], \tag{41b}$$

$$\Delta_{uav}[n] \le \Delta t V_{max}, \tag{41c}$$

$$\Delta_{uav}[n] \le \theta H, \tag{41d}$$

$$\sum_{n=1}^{N} R_i[n]\Delta t \ge B_i, \tag{41e}$$

where the numerator of (41a) is non-concave, $E_{uNcvx}(\Delta t)$ is non-convex, and (41e) is non-concave with respect to $\mathbf{w}$. Thus, we need to transform them into a mathematically solvable problem. The first-order Taylor expansion is utilized to change them into a mathematically solvable convex expression.

First, $R_i[n]$ can be expanded at a given point $w^{(r)}[n]$ to

$$R_i[n] \ge R_i^{lb}[n], \tag{42}$$

where

$$\begin{aligned} R_i^{lb}[n] = R_i^{(0)}[n] + R_i^{(1)}[n] \Big(&\|w[n] - L_i\|^\alpha \\ &- \|w^{(r)}[n] - L_i\|^\alpha \Big). \end{aligned} \tag{43}$$

$w^{(r)}[n]$ is assumed to be the optimal value of $w[n]$ in (41) from the r-th iteration, and $R_i^{(0)}[n] = R_i[n](w^{(r)}[n])$. $R_i^{(1)}[n]$ is the first-order derivative of $R_i[n]$ with respect to $\|\|w[n] - Li\|\|^\alpha$, which can be derived as

$$\begin{aligned} R_i^{(1)}[n] &= \frac{\partial R_i[n]}{\partial \|w^{(r)}[n] - L_i\|^\alpha} \\ &= t_i[n] \left[\frac{\frac{\partial \gamma_i^{(r)}[n]}{\partial \left(\|w^{(r)}[n] - L_i\|^\alpha \right)}}{(1 + \gamma_i^{(r)}[n]) \ln 2} - \frac{\frac{Q^{-1}(\epsilon) \partial V_i^{(r)}[n]}{\partial \left(\|w^{(r)}[n] - L_i\|^\alpha \right)}}{2 \ln 2 \sqrt{M V_i^{(r)}[n]}} \right], \end{aligned} \tag{44}$$

where

$$\frac{\partial \gamma_i^{(r)}[n]}{\partial\left(\|w^{(r)}[n]-L_i\|^{\alpha}\right)}=\frac{-P_s\rho_0}{\sigma^2\left(\|w^{(r)}[n]-L_i\|^{\alpha}\right)}, \tag{45}$$

and

$$\frac{\partial V_i^{(r)}[n]}{\partial\left(\|w^{(r)}[n]-L_i\|^{\alpha}\right)}=\frac{-2P_s\rho_0}{\sigma^2(1+\gamma_i^{(r)}[n])^3\left(\|w^{(r)}[n]-L_i\|^{\alpha}\right)}. \tag{46}$$

Then, (41e) can be changed into

$$\sum_{n=1}^{N} R_i[n]\Delta t \geq \sum_{n=1}^{N} R_i^{lb}[n]\Delta t \geq B_i, \tag{47}$$

Similar to (32), we have

$$\frac{\Delta t^4}{z[n]^2} \leq z[n]^2+\frac{\Delta_{uav}[n]^2}{\bar{v}^2}, \tag{48}$$

where the right hand is non-concave with respect to $z[n]$, which can be expanded into

$$\begin{aligned} &z[n]^2+\frac{\Delta_{uav}[n]^2}{\bar{v}^2} \\ &\quad\geq \left(z^{(r)}[n]\right)^2+2\, z^{(r)}[n]\left(z[n]-z^{(r)}[n]\right) \\ &\qquad+\frac{2}{\bar{v}^2}\left(w^{(r)}[n]-w^{(r)}[n-1]\right)^T(w[n]-w[n-1]) \\ &\qquad-\frac{\|w^{(r)}[n]-w^{(r)}[n-1]\|^2}{\bar{v}^2} \geq \frac{\Delta t^4}{\bar{v}^2}. \end{aligned} \tag{49}$$

In (49), $z^{(r)}[n]$ is assumed to be the optimal value of $z[n]$ in (41) from the r-th iteration.

Finally, (41) can be changed into a mathematically solvable problem as

$$\textbf{P1.2.a:}\quad \max_{\mathbf{w},z[n]} \frac{\sum_{i=1}^{S}\sum_{n=1}^{N} R_i^{lb}[n]\Delta t}{E_{ucvx}(\Delta t)+P_{ind}\sum_{n=1}^{N} z[n]} \tag{50a}$$

$$s.t.\ w[1]=w[N], \tag{50b}$$

$$\Delta_{uav}[n] \leq \Delta t V_{max}, \tag{50c}$$

$$\Delta_{uav}[n] \leq \theta H, \tag{50d}$$

$$\sum_{s=1}^{S}\sum_{n=1}^{N} R_i^{lb}[n]\Delta t \geq B_i, \tag{50e}$$

$$\begin{aligned} &\frac{2}{\bar{v}^2}\left(w^{(r)}[n]-w^{(r)}[n-1]\right)^T(w[n]-w[n-1]) \\ &\quad+\left(z^{(r)}[n]\right)^2+2\, z^{(r)}[n]\left(z[n]-z^{(r)}[n]\right) \\ &\quad-\frac{\|w^{(r)}[n]-w^{(r)}[n-1]\|^2}{\bar{v}^2} \geq \frac{\Delta t^4}{\bar{v}^2}, \end{aligned} \tag{50f}$$

which can be solved by existing convex programming tools such as CVX.

Then, the optimal trajectory $\mathbf{w}^*$, flight duration T^*, and scheduling vector $\mathbf{t}^*$ can be obtained by iteratively solving P1.1.b and P1.2.a.

Accordingly, Algorithm 1 is summarized to solve P1.

The computational complexity of the proposed scheme can be concluded as follows. There are $N-1$ linear matrix inequalities (LMI) of dimension 1, N LMI of dimension 1, $2S$ LMI of dimension N, I LMI of dimension 1, I LMI of dimension 1, N LMI of dimension 1, S second-order cones (SOC) of dimension 3, and S SOC of dimension 2 in Step 4. In addition, the total number of variables is $2S+N+1$. Then, the number of iterations is $\mathcal{O}(SN)$, and the complexity of each is $\mathcal{O}\left(N^2S(N^2+S^2+SN)\right)$. Accordingly, the total computational complexity of Step 4 is $\mathcal{O}\left(N^{4.5}S^{1.5}+N^{2.5}S^{3.5}+N^{3.5}S^{2.5}\right)$. Similarly, the computational complexity of Step 5 can be calculated as $\mathcal{O}\left(\sqrt{N+S}(N^3+SN^2)\right)$. Thus, the overall computational complexity of Algorithm 1 can be expressed as $\mathcal{O}\left(N^{4.5}S^{1.5}+N^{2.5}S^{3.5}+N^{3.5}S^{2.5}\right)$.

Algorithm 1 Iterative Algorithm to Solve P1

1: **Initialization** Initialize $\mathbf{w}^{(0)}, \mathbf{t}^{(0)}, \Delta t^{(0)}$.
2: Set iteration index $r=0$.
3: **repeat**
4: Obtain $\mathbf{t}^{(r+1)}$ and $\Delta t^{(r+1)}$ from (40), under the given $\mathbf{w}^{(r)}$.
5: Obtain $\mathbf{w}^{(r+1)}$ from (50), under the given $\mathbf{t}^{(r+1)}$ and $\Delta t^{(r+1)}$.
6: Set $r=r+1$.
7: **until** Convergence
8: Set $\mathbf{t}^*=\mathbf{t}^{(r)}$, $\Delta t^*=\Delta t^{(r)}$, and $\mathbf{w}^*=\mathbf{w}^{(r)}$.

IV. Secrecy Rate Maximization

During the data collection, the UAV also transfers the received data from the sensors together with its own data to the BS. Meanwhile, it should prevent the adversarial eavesdropping, with the secrecy outage probability requirement satisfied. Therefore, we should optimize the transmit power P_a and the information blocklength N_u to maximize the secrecy rate, while keeping the secrecy outage probability and the eavesdropping rate lower than the constraints.

Thus, the optimization can be formulated as

$$\textbf{P2:}\quad \max_{P_a,N_u} \sum_{n=1}^{N} R_s[n] \tag{51a}$$

$$s.t.\ P_a \leq P_{a_{max}}, \tag{51b}$$

$$N_u \leq N_{u_{max}}, \tag{51c}$$

$$R_e[n] \leq r, \tag{51d}$$

$$p_{out}[n] \leq \xi, \tag{51e}$$

where $P_{a_{max}}$ is the maximum allowed transmit power of UAV, $N_{u_{max}}$ represents the maximum allowed information blocklength, and r and ξ denote the thresholds of eavesdropping rate and outage probability, respectively.

The environmental noise is usually smaller than the signal power. In the rest of this paper, we consider the large SNR situation, where both $\sqrt{\frac{\gamma_b[n](\gamma_b[n]+2)}{(\gamma_b[n]+1)^2}}$ and $\sqrt{\frac{\gamma_e[n](\gamma_e[n]+2)}{(\gamma_e[n]+1)^2}}$ approach to 1. Thus, we have

$$R_s[n] \geq \log_2\left(\frac{1+\gamma_b[n]}{1+\gamma_e[n]}\right)-\frac{Q^{-1}(\epsilon)+Q^{-1}(\delta_e)}{\ln 2\sqrt{N_u}}=\tilde{R}_s[n]. \tag{52}$$

Then, the expression of $p_{out}[n]$ is derived in Proposition 1.

Proposition 1: The detailed expression of $p_{out}[n]$ in (25) follows

$$p_{out}[n] = \int_{f(P_a)}^{+\infty} \frac{1}{a^2} \mathrm{e}^{-\frac{q[n]+b^2}{a^2}} I_0\left(\frac{b\sqrt{q[n]}}{a^2}\right) dq[n]. \tag{53}$$

Proof: The $p_{out}[n]$ defined in (25) can be changed into (54), as shown at the bottom of the next page, where $q[n] = |\mathbf{h}_e[n]\mathbf{u}[n]|^2$, and $f(P_a)$ can be expressed as

$$f(P_a) = \frac{\sigma^2 d_e[n]^\alpha \left(2^{\log_2\left(1+\frac{MP_a\rho_0}{\sigma^2 d_b[n]^\alpha}\right) - \frac{Q^{-1}(\epsilon)+Q^{-1}(\delta_e)}{\ln 2\sqrt{N_u}} - R_0[n]} - 1\right)}{P_a\rho_0}. \tag{55}$$

Since $c_L\mathbf{h}_{eL}[n]\mathbf{u}[n]$ in $q[n]$ is a constant while $c_N\mathbf{h}_{eN}[n]\mathbf{u}[n]$ is a random variable, we transform $q[n]$ for analysis simplicity as

$$q[n] = |ax + b]|^2, \tag{56}$$

where $b = c_L\mathbf{h}_{eL}[n]\mathbf{u}[n]$, $a = c_N$, and $x = \mathbf{h}_{eN}[n]\mathbf{u}[n]$. It is proved in [30] that $\mathbf{h}_{eN}[n]\mathbf{u}[n] \sim \mathcal{CN}(0,1)$. According to [31], $q[n] \sim \chi^2(2, b^2)$ and the probability density function of $q[n]$ can be expressed as

$$f_q(q[n]) = \frac{1}{a^2} \mathrm{e}^{-\frac{q[n]+b^2}{a^2}} I_0\left(\frac{b\sqrt{q[n]}}{a^2}\right). \tag{57}$$

Therefore, $p_{out}[n]$ in (54) can be changed into (53). Proposition 1 is proved. ∎

Then, since the trajectory is optimized in P1, the maximization of $\sum_{n=1}^{N} R_s[n]$ is equivalent to maximizing each $\tilde{R}_s[n]$. Thus, P2 can be reformulated into

$$\textbf{P2.1:} \quad \max_{P_a, N_u} \ \tilde{R}_s[n] \tag{58a}$$
$$s.t. \ P_a \le P_{a_{max}}, \tag{58b}$$
$$N_u \le N_{u_{max}}, \tag{58c}$$
$$R_e[n] \le r, \tag{58d}$$
$$p_{out}[n] \le \xi. \tag{58e}$$

To derive the optimal transmit power P_a^* of UAV and the optimal blocklength N_u^*, we analyze the monotonicity of $\tilde{R}_s[n]$, $R_e[n]$, and $p_{out}[n]$ with respect to P_a and N_u in the following propositions.

Proposition 2: $\tilde{R}_s[n]$ monotonically increases with respect to P_a and N_u.

Proof: From the expression in (52), we have the first-order derivative of $\tilde{R}_s[n]$ with respect to P_a as

$$\frac{\partial \tilde{R}_s[n]}{\partial P_a} = \frac{M\rho_0/\ln 2}{(d_b[n]^\alpha\sigma^2 + MP_a\rho_0)} - \frac{|\mathbf{h}_e\mathbf{u}|^2\rho_0/\ln 2}{(d_e[n]^\alpha\sigma^2 + |\mathbf{h}_e\mathbf{u}|^2 P_a\rho_0)} = \frac{\rho_0\sigma^2\left(d_e[n]^\alpha M - |\mathbf{h}_e\mathbf{u}|^2 d_b[n]^\alpha\right)/\ln 2}{(d_b[n]^\alpha\sigma^2 + MP_a\rho_0)(d_e[n]^\alpha\sigma^2 + |\mathbf{h}_e\mathbf{u}|^2 P_a\rho_0)}. \tag{59}$$

With the definition of each parameter in (59), it is easy to conclude $\frac{\partial \tilde{R}_s[n]}{\partial P_a} > 0$, which indicates that $\tilde{R}_s[n]$ monotonically increases with the transmit power P_a at the UAV.

In addition, we have the first-order derivative of $\tilde{R}_s[n]$ with respect to N_u as

$$\frac{\partial \tilde{R}_s[n]}{\partial N_u} = \frac{Q^{-1}(\epsilon) + Q^{-1}(\delta)N^{-\frac{3}{2}}}{2\ln 2} > 0, \tag{60}$$

from which, we can conclude that $\tilde{R}_s[n]$ monotonically increases with N_u.

Proposition 2 is proved. ∎

Therefore, to achieve higher $\tilde{R}_s[n]$, we need to set larger N_u and P_a. Then, the first-order derivative of eavesdropping rate $R_e[n]$ with respect to P_a and N_u is analyzed in Proposition 3.

Proposition 3: $R_e[n]$ monotonically increases with P_a and N_u.

Proof: First, in the large SNR scenario, the first-order derivative of eavesdropping rate $R_e[n]$ with respect to P_a can be derived as

$$\frac{\partial R_e[n]}{\partial P_a} = \frac{\rho_0|\mathbf{h}_e[n]\mathbf{u}[n]|^2}{(1+\gamma_e[n])\ln 2\ d_e[n]^\alpha} > 0. \tag{61}$$

Then, the first-order derivative of eavesdropping rate $R_e[n]$ with respect to N_u can be derived as

$$\frac{\partial R_e[n]}{\partial N_u} = \frac{Q^{-1}(\delta)}{2\ln 2} N_u^{-\frac{3}{2}} > 0. \tag{62}$$

Thus, we can conclude that the increase of P_a and N_u will both result in a larger $R_e[n]$.

Proposition 3 is proved. ∎

Furthermore, we have the first-order derivative of $p_{out}[n]$ with respect to P_a and N_u in Proposition 4.

Proposition 4: $p_{out}[n]$ monotonicially decreases with P_a and N_u.

Proof: The first-order derivative of $R_e[n]$ with respect to P_a can be described as

$$\frac{\partial p_{out}[n]}{\partial P_a} = -\frac{\mathrm{e}^{-\frac{f(P_a)+b^2}{a^2}} I_0\frac{b\sqrt{f(P_a)}}{a^2}}{a^2} \frac{\partial f(P_a)}{\partial P_a}, \tag{63}$$

where we can derive the first-order derivative of $f(P_a)$ with respect to P_a from (55) as

$$\frac{\partial f(P_a)}{\partial P_a} = \frac{\left(2^{c[n]}\left[\frac{\ln c[n] MP_a\rho_0}{(d_b[n]^\alpha\sigma^2 + MP_a\rho_0)\ln 2} - 1\right] + 1\right)\sigma^2 d_e[n]^\alpha}{P_a^2\rho_0} \ge \frac{\frac{\ln c[n] MP_a\rho_0}{(d_b[n]^\alpha\sigma^2 + MP_a\rho_0)\ln 2}\sigma^2 d_e[n]^\alpha}{P_a^2\rho_0} > 0, \tag{64}$$

where

$$c[n] = \log_2\left(1 + \frac{MP_a\rho_0}{\sigma^2 d_b[n]^\alpha}\right) - \frac{Q^{-1}(\epsilon) + Q^{-1}(\delta_e)}{\ln 2\sqrt{N_u}} - R_0[n]. \tag{65}$$

From (63) and (64), we can see that $\frac{\partial p_{out}[n]}{\partial P_a} < 0$, which indicates that $p_{out}[n]$ monotonically decreases with P_a. Thus, to achieve a smaller $p_{out}[n]$, we need to increase the transmit power at the UAV.

Besides, we have the first-order derivative of $p_{out}[n]$ with respect to N_u as

$$\frac{\partial p_{out}[n]}{\partial N_u} = -\frac{\mathrm{e}^{-\frac{g(N_u)+b^2}{a^2}} I_0\left(\frac{b\sqrt{g(N_u)}}{\sigma^2}\right)}{a^2} \frac{\partial g(N_u)}{\partial N_u}, \tag{66}$$

where we set $g(N_u) = f(P_a)$. $\frac{\partial g(N_u)}{\partial N_u}$ can be derived as

$$\frac{\partial g(N_u)}{\partial N_u} = 2^{c[n]} \ln 2 \frac{Q^{-1}(\epsilon) + Q^{-1}(\delta_e)}{2 \ln 2} N_u^{-\frac{3}{2}} > 0. \quad (67)$$

Thus, we can conclude that $\frac{\partial p_{out}[n]}{\partial N_u} < 0$, which indicates that we should increase N_u to achieve a smaller secrecy outage probability $p_{out}[n]$.

Proposition 4 is proved. ■

Then, the solution to P2.1 can be derived in Proposition 5.

Proposition 5: The optimal transmit power P_a^* and blocklength N_u^* at the UAV for P2.1 can be derived as

$$P_a^* = \min\left\{P_{a_{max}}, \bar{R}_e[n]^{-1}(N_u^*, r)\right\}, \quad (68)$$

where N_u^* can be derived via the traversal algorithm to maximize $\tilde{R}_s[n](P_a^{N_u}, N_u)$.

Proof: To satisfy (58d), we need to keep the transmit power P_a and the blocklength N_u small. However, the decrease of both P_a and N_u will result in the decrease of $\tilde{R}_s[n]$ and the increase of $p_{out}[n]$. Therefore, we set P_a and N_u as large as possible with (58d) satisfied.

We first derive the upper bounds of P_a and N_u with (58d) taking the equality, and then figure out the optimal pair of (P_a^*, N_u^*) to maximize $\tilde{R}_s[n]$ while guaranteeing (58e). However, there exists a trade-off between P_a and N_u owing to that both of their increase can improve the performance. Since N_u is an integer, we derive the expression of the upper bound of P_a from $R_e[n] = r$ as $P_a^{N_u} = R_e[n]^{-1}(N_u, r)$, where $R_e[n]^{-1}(*)$ is the inverse function of $R_e[n]$. However, since we cannot obtain $\mathbf{h}_e[n]$ in $R_e[n]$, we replace $R_e[n]$ with its mean value of $\bar{R}_e[n]$. Thus, $P_a^{N_u}$ can be derived as

$$P_a^{N_u} = \bar{R}_e[n]^{-1}(N_u, r). \quad (69)$$

Proposition 5 is proved. ■

Remark: According to (68), P_a should be reduced to $P_{a_{max}}$ when $\bar{R}_e[n]^{-1}(N_u^*, r) > P_{a_{max}}$. Then, N_u^* should also be adjusted accordingly by maximizing $\tilde{R}_s[n](P_{a_{max}}, N_u)$.

V. Simulation Results and Discussion

Simulation results are provided to demonstrate the effectiveness of the proposed scheme. There are six sensors randomly distributed within a square ground with each side of 1500 m. The UAV is flying above the square area with a fixed altitude $H = 100$ m. The maximum velocity of UAV is set as $V_{max} = 50$ m/s, and the flight duration T is divided into $N = 60$ time slots. For the aerodynamic propulsion parameters of UAV, the profile power of blades $P_{bld} = 79.86$ W, the tip speed of rotor blades $v_t = 120$ m/s, the fuselage drag ratio $r_{drag} = 0.6$, the density of air $\rho_{air} = 1.225$ kg/m^3, the solidity of rotor $h_{rtor} = 0.05$, the disc area of rotor $S_{rtor} = 0.50$ m^2, the induced power $P_{ind} = 88.61$ W when $\frac{\Delta uav[n]}{\Delta t} = 0$, and the mean induced speed of motor $\bar{v} = 4.03$ m/s according to [32]. The number of antennas at the UAV is set to $M = 8$. Assume that the BS locates at $L_b(7000, 0, 100)$ and the estimated closest location of eavesdropper is at $L_e(7500, 0, 0)$ in meters. In addition, the environmental noise power variance is set as $\sigma^2 = -110$ dBm. The large-scale channel fading reference at 1 m can be set to $\rho_0 = 10^{-6}$. The channel fading parameters are assumed as $K = 5$ and $\alpha = 2$. According to [33], $N_u > 100$ is usually set. In the simulation, we also examine the case when $N_u < 100$ to show the influence of blocklength.

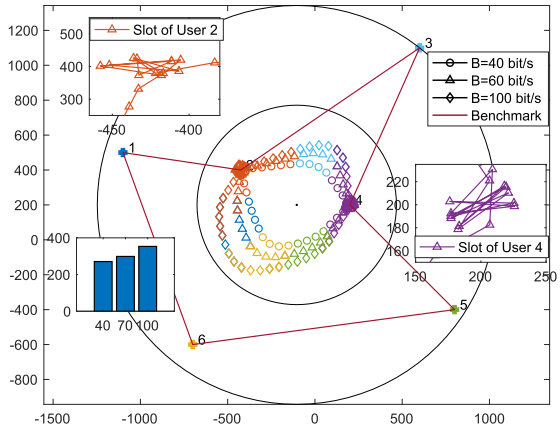

Fig. 2. Comparison of trajectories under different minimum collected data B_i of the proposed scheme and the benchmark.

A. Data Collection Phase

The trajectories of UAV are compared in Fig. 2, when the lower bound of collected data for each sensor is set to $B_i = 40$ bit/Hz, $B_i = 60$ bit/Hz, $B_i = 80$ bit/Hz in the proposed EE algorithm, and $B_i = 40$ bit/Hz for the benchmark, respectively. The transmit power P_s at each sensor is set to 0.1 W. The proposed scheme focuses more on the EE. In the benchmark, the UAV boosts to its maximum velocity V_{max} to fly to each sensor and then hovers above it to collect 40 bit/Hz data in each round. We use different colors to represent the time slots assigned to different users during the collection. From the results, we can see that the trajectories of the proposed scheme in different settings tend to be shorter, and the UAV tends to hover above the two central users for a longer time. This is because a shorter path can reduce the energy consumption of UAV and thus increase EE. Hovering around the centered users can also save energy. In addition, we can see that the UAV tends to fly closer to other edge users when B_i increases.

In Fig. 3, the EE r_{tc} and sum collected data are compared between the proposed EE scheme and the benchmark with different B_i. The transmit power P_s in each scheme is set as 0.1 W. From the results, we can see that the proposed scheme is superior in both EE and collected data. Specifically, the collected data of both schemes increase with B_i. On the other hand, the EE of the proposed scheme decreases with B_i while that of the benchmark monotonically increases with B_i. This is because higher data requirement results in a longer flight duration for the proposed scheme, which increases the energy consumption of UAV and thus reduces the EE.

$$p_{out}[n] = Pr\left(\log_2\left(1+\frac{MP_a\rho_0}{\sigma^2 d_b[n]^\alpha}\right) - \frac{Q^{-1}(\epsilon)+Q^{-1}(\delta_e)}{\ln 2\sqrt{N_u}} - \log_2\left(1+\frac{P_a\rho_0}{\sigma^2 d_e[n]^\alpha}q[n]\right) \le R_0[n]\right) = Pr\left(q[n] \ge f(P_a)\right). \quad (54)$$

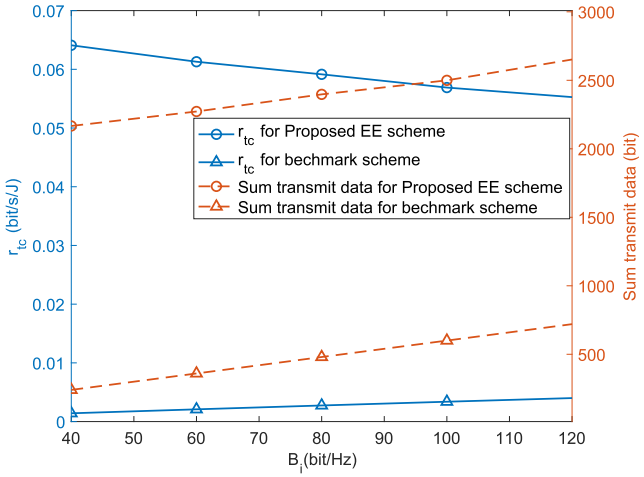

Fig. 3. Comparison of EE and sum collected data between the proposed scheme and the benchmark with different B_i.

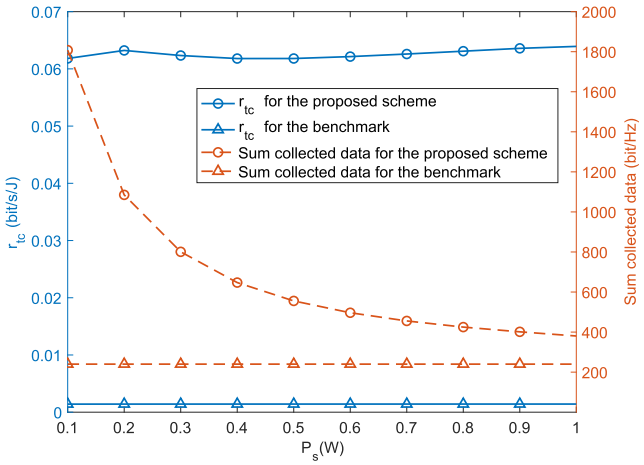

Fig. 4. Comparison of EE and sum collected data between the proposed scheme and the benchmark with different transmit power P_s at the sensors.

The impacts of the transmit power P_s at each sensor on the EE and collected data are plotted in Fig. 4, where the proposed scheme is compared to the benchmark. The minimum collected data in both schemes is set as $B_i = 40$ bit/Hz. From the results, we can observe that regardless of the values of transmit power P_s, the proposed scheme can achieve better performance of both EE and collected data. Moreover, the collected data of the proposed scheme decreases with the incremental of the transmit power P_s. This is due to the fact that the increase of P_s of each sensor results in a higher transmission rate, which can satisfy the minimum collected data B_i with a shorter flight duration.

B. Short-Packet Transmission Phase

Fig. 5 shows the impact of P_a on the average achievable eavesdropping rate R_e, transmission rate R_b and secrecy rate R_s. We set $B_i = 40$ bit/s, $P_s = 0.1$ W and $N_u = 20$. From the results, we can see that although the eavesdropping rate R_e increases with P_a, the transmission rate R_b towards the BS increases more rapidly, which enables the secrecy rate R_s to increase with P_a. This is because the MRT can result in higher SINR at the legitimate receiver.

The impacts of the blocklength N_u on R_b, R_e, and R_s are investigated in Fig. 6. We have $P_s = 0.1$ W, $B_i = 40$ bit/Hz and $P_a = 0.1$ W. From the results, we can see that R_e, R_b,

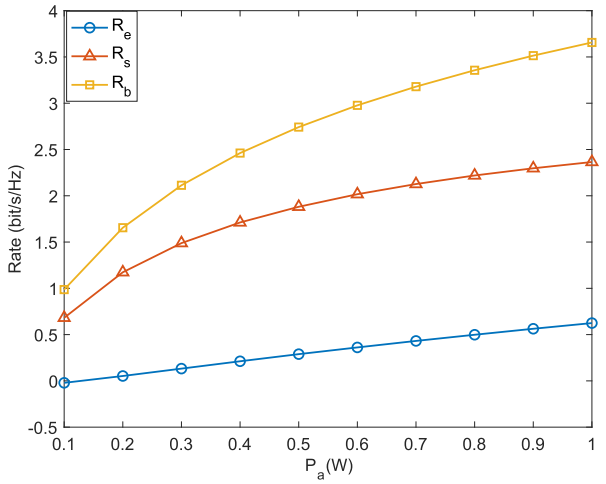

Fig. 5. Comparison of the average achievable eavesdropping rate R_e, transmission rate R_b and secrecy rate R_s with different transmit power P_a of UAV.

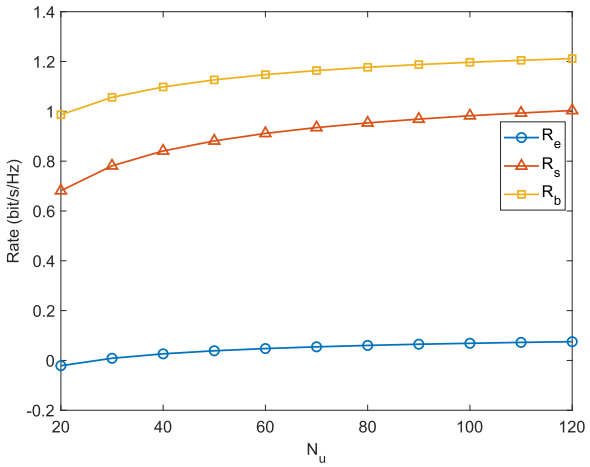

Fig. 6. Comparison of the average achievable eavesdropping rate R_e, transmission rate R_b and secrecy rate R_s with different blocklength N_u.

and R_s all increase with the blocklength N_u. This is because the MRT can bring a higher SINR at BS, which enables R_b to increase faster than R_e.

Then, the impact of P_a and N_u on the secrecy outage propability p_{out} is shown in Fig. 7. We have $P_s = 0.1$ W, $B_i = 40$ bit/Hz and $R_0[n] = 1.8$ bit/s/Hz. From the results, we can see that the secrecy outage probability p_{out} decreases with P_a. In addition, the increase of N_u can also lead to the reduction of p_{out}. Thus, a smaller p_{out} can be achieved by either a higher P_a or a larger N_u.

Finally, the impacts of the blocklength N_u and eavesdropping rate threshold r on the maximum achievable secrecy rate R_s and R_b are investigated in Fig. 8. We have $B_i = 40$ bit/s and $P_s = 0.1$ W. The transmit power P_a^* is derived from (68). From the results, we can see that R_b decreases with N_u with a given r, which indicates that the optimal transmit power P_a also decreases with N_u. This is because there is a trade-off between the maximum allowed transmit power P_a and the blocklength N_u under a given threshold r. In addition, the maximum achievable R_s first increases with N_u sharply, and then reaches a saturation level. This is because increasing the blocklength can enlarge the achievable secrecy rate, however, bounded by Shannon capacity. To evaluate the effectiveness

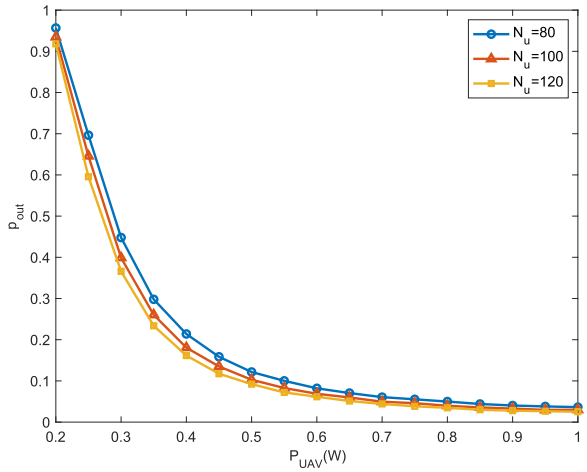

Fig. 7. Comparison of the secrecy outage probability p_{out} with different transmit power P_a. Different values of blocklength $N_u = 80$, $N_u = 100$, $N_u = 120$ are considered.

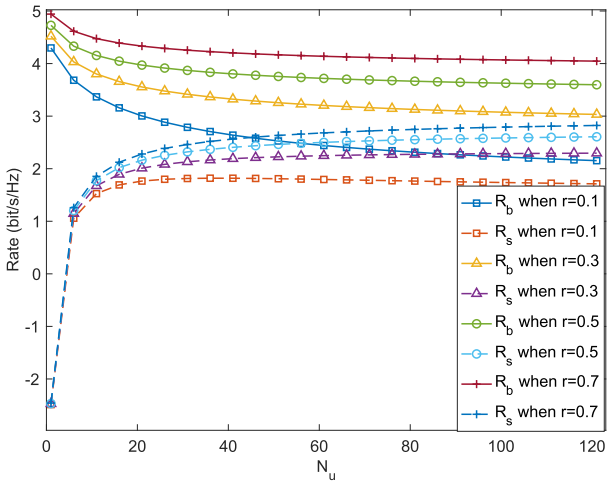

Fig. 8. Comparison of the maximum achievable R_s and R_b with different blocklength N_u. Four cases of $r = 0.1$ bit/s/Hz, $r = 0.3$ bit/s/Hz, $r = 0.5$ bit/s/Hz, $r = 0.7$ bit/s/Hz are considered.

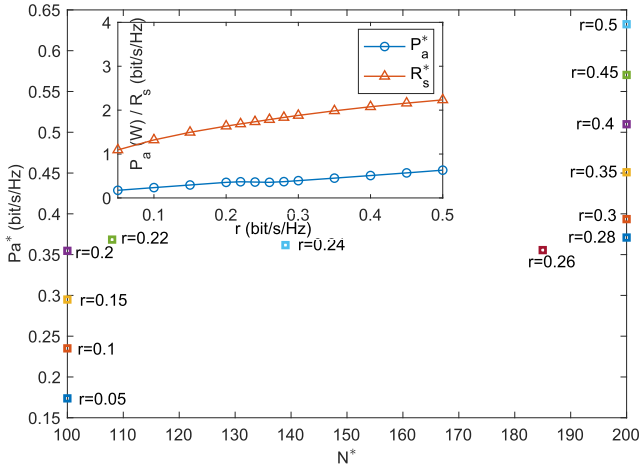

Fig. 9. Comparison of the maximum achievable R_s and the corresponding P_a^* and N_u^* under different values of r.

of the proposed scheme, we investigate the optimized P_a^* and N_u^* under different values of the eavesdropping rate threshold r in Fig. 9, where $100 \leq N_u \leq 200$. From the results, we can see that P_a^* increases as r, while N_u^* equaling to the smallest value when r is small but increases when r gets bigger. This indicates that N_u has more impact on R_e compared with R_b when r is small, and smaller N_u can achieve larger R_s. However, larger N_u is preferred when r increases.

VI. Conclusion

A secure short-packet data collection and transmission scheme for UAV-assisted wireless networks has been proposed in this paper. First, the trajectory together with the flight duration of UAV and the user scheduling are jointly designed to maximize the EE in the data collection phase. The formulated optimization problem is non-convex and mathematically unsolvable. We utilize the first-order Taylor expansion to convert it to two convex subproblems, which are solved via SCA. Then, in the data transmission phase, with the derived optimal trajectory of UAV, we optimize the transmit power and the blocklength of the secure short-packet transmission from the UAV to BS against the malicious eavesdropping to achieve a maximum secrecy rate while guaranteeing the reliability. Finally, simulation results are presented to evaluate the effectiveness of the proposed scheme.

References

[1] X. Chen, Z. Chang, N. Zhao, T. Hamalainen, and X. Wang, "Energy-efficient secure data collection and transmission via UAV," in *Proc. IEEE Global Commun. Conf. (GLOBECOM)*, Dec. 2022, pp. 1–6.

[2] K. David and H. Berndt, "6G vision and requirements: Is there any need for beyond 5G?" *IEEE Veh. Technol. Mag.*, vol. 13, no. 3, pp. 72–80, Sep. 2018.

[3] J. Liu, Y. Shi, Z. M. Fadlullah, and N. Kato, "Space-air-ground integrated network: A survey," *IEEE Commun. Surveys Tuts.*, vol. 20, no. 4, pp. 2714–2741, 4th Quart., 2018.

[4] Y. Zeng, R. Zhang, and T. J. Lim, "Wireless communications with unmanned aerial vehicles: Opportunities and challenges," *IEEE Commun. Mag.*, vol. 54, no. 5, pp. 36–42, May 2016.

[5] Y. Liu, Z. Qin, Y. Cai, Y. Gao, G. Y. Li, and A. Nallanathan, "UAV communications based on non-orthogonal multiple access," *IEEE Wireless Commun.*, vol. 26, no. 1, pp. 52–57, Feb. 2019.

[6] L. Gupta, R. Jain, and G. Vaszkun, "Survey of important issues in UAV communication networks," *IEEE Commun. Surveys Tuts.*, vol. 18, no. 2, pp. 1123–1152, 2nd Quart. 2016.

[7] B. Mao, F. Tang, Y. Kawamoto, and N. Kato, "Optimizing computation offloading in satellite-UAV-Served 6G IoT: A deep learning approach," *IEEE Netw.*, vol. 35, no. 4, pp. 102–108, Aug. 2021.

[8] L. Zhang, Y.-C. Liang, and D. Niyato, "6G visions: Mobile ultra-broadband, super Internet-of-Things, and artificial intelligence," *China Commun.*, vol. 16, no. 8, pp. 1–14, Aug. 2019.

[9] H. Guo and J. Liu, "UAV-enhanced intelligent offloading for Internet of Things at the edge," *IEEE Trans. Ind. Informat.*, vol. 16, no. 4, pp. 2737–2746, Apr. 2020.

[10] W. Wang, N. Zhao, L. Chen, X. Liu, Y. Chen, and D. Niyato, "UAV-assisted time-efficient data collection via uplink NOMA," *IEEE Trans. Commun.*, vol. 69, no. 11, pp. 7851–7863, Nov. 2021.

[11] J. Liu, P. Tong, X. Wang, B. Bai, and H. Dai, "UAV-aided data collection for information freshness in wireless sensor networks," *IEEE Trans. Wireless Commun.*, vol. 20, no. 4, pp. 2368–2382, Apr. 2021.

[12] Y. Liu, K. Xiong, Y. Lu, Q. Ni, P. Fan, and K. B. Letaief, "UAV-aided wireless power transfer and data collection in Rician fading," *IEEE J. Sel. Areas Commun.*, vol. 39, no. 10, pp. 3097–3113, Oct. 2021.

[13] R. Zhang, X. Pang, W. Lu, N. Zhao, Y. Chen, and D. Niyato, "Dual-UAV enabled secure data collection with propulsion limitation," *IEEE Trans. Wireless Commun.*, vol. 20, no. 11, pp. 7445–7459, Nov. 2021.

[14] H. Yang, J. Zhao, Z. Xiong, K.-Y. Lam, S. Sun, and L. Xiao, "Privacy-preserving federated learning for UAV-enabled networks: Learning-based joint scheduling and resource management," *IEEE J. Sel. Areas Commun.*, vol. 39, no. 10, pp. 3144–3159, Oct. 2021.

[15] X. Xu, H. Zhao, H. Yao, and S. Wang, "A blockchain-enabled energy-efficient data collection system for UAV-assisted IoT," *IEEE Internet Things J.*, vol. 8, no. 4, pp. 2431–2443, Feb. 2021.

[16] Y. Xu, T. Zhang, D. Yang, Y. Liu, and M. Tao, "Joint resource and trajectory optimization for security in UAV-assisted MEC systems," *IEEE Trans. Commun.*, vol. 69, no. 1, pp. 573–588, Jan. 2021.

[17] X. Chen et al., "Secure transmission via power allocation in NOMA-UAV networks with circular trajectory," *IEEE Trans. Veh. Technol.*, vol. 69, no. 9, pp. 10033–10045, Sep. 2020.
[18] W. Wang et al., "Joint precoding optimization for secure SWIPT in UAV-aided NOMA networks," *IEEE Trans. Commun.*, vol. 68, no. 8, pp. 5028–5040, Aug. 2020.
[19] C. Zhong, J. Yao, and J. Xu, "Secure UAV communication with cooperative jamming and trajectory control," *IEEE Commun. Lett.*, vol. 23, no. 2, pp. 286–289, Feb. 2019.
[20] J. Kang, Z. Xiong, D. Niyato, S. Xie, and D. I. Kim, "Securing data sharing from the sky: Integrating blockchains into drones in 5G and beyond," *IEEE Netw.*, vol. 35, no. 1, pp. 78–85, Jan. 2021.
[21] D. Xu and P. Ren, "Quantum learning based nonrandom superimposed coding for secure wireless access in 5G URLLC," *IEEE Trans. Inf. Forensics Security*, vol. 16, pp. 2429–2444, 2021.
[22] H. Ji, S. Park, J. Yeo, Y. Kim, J. Lee, and B. Shim, "Ultra-reliable and low-latency communications in 5G downlink: Physical layer aspects," *IEEE Wireless Commun.*, vol. 25, no. 3, pp. 124–130, Jun. 2018.
[23] Z. Zhu et al., "Research and analysis of URLLC technology based on artificial intelligence," *IEEE Commun. Standards Mag.*, vol. 5, no. 2, pp. 37–43, Jun. 2021.
[24] X. Yang, Z. Zho, and B. Huang, "URLLC key technologies and standardization for 6G power Internet of Things," *IEEE Commun. Standards Mag.*, vol. 5, no. 2, pp. 52–59, Jun. 2021.
[25] A. Ranjha and G. Kaddoum, "URLLC facilitated by mobile UAV relay and RIS: A joint design of passive beamforming, blocklength, and UAV positioning," *IEEE Internet Things J.*, vol. 8, no. 6, pp. 4618–4627, Mar. 2021.
[26] H. Ren, C. Pan, K. Wang, Y. Deng, M. Elkashlan, and A. Nallanathan, "Achievable data rate for URLLC-enabled UAV systems with 3-D channel model," *IEEE Wireless Commun. Lett.*, vol. 8, no. 6, pp. 1587–1590, Jul. 2019.
[27] C. Pan, H. Ren, Y. Deng, M. Elkashlan, and A. Nallanathan, "Joint blocklength and location optimization for URLLC-enabled UAV relay systems," *IEEE Commun. Lett.*, vol. 23, no. 3, pp. 498–501, Mar. 2019.
[28] W. Yang, R. F. Schaefer, and H. V. Poor, "Wiretap channels: Nonasymptotic fundamental limits," *IEEE Trans. Inf. Theory*, vol. 65, no. 7, pp. 4069–4093, Jul. 2019.
[29] S. Boyd, S. P. Boyd, and L. Vandenberghe, *Convex Optimization*. Cambridge, U.K.: Cambridge Univ. Press, 2004.
[30] X. Chen et al., "Multi-antenna covert communication via full-duplex jamming against a warden with uncertain locations," *IEEE Trans. Wireless Commun.*, vol. 20, no. 8, pp. 5467–5480, Aug. 2021.
[31] S. I. Resnick, *Adventures in Stochastic Processes*. New York, NY, USA: Springer, 1992.
[32] Y. Zeng, J. Xu, and R. Zhang, "Energy minimization for wireless communication with rotary-wing UAV," *IEEE Trans. Wireless Commun.*, vol. 18, no. 4, pp. 2329–2345, Apr. 2019.
[33] Y. Polyanskiy, H. V. Poor, and S. Verdú, "Channel coding rate in the finite blocklength regime," *IEEE Trans. Inf. Theory*, vol. 56, no. 5, pp. 2307–2359, May 2010.

Xinying Chen received the B.E. degree in electronic information engineering from the Dalian University of Technology, China, in 2015, and the M.S. degree in communication engineering from the Beijing University of Posts and Telecommunications in 2018. She is currently working toward a Ph.D. degree in software and communication engineering with the University of Jyväskylä, Finland. She also works on a Ph.D. degree in information and telecommunication engineering with the Dalian University of Technology. Her research interests include covert communications, physical-layer security in NOMA, and URLLC security.

Nan Zhao (Senior Member, IEEE) received the Ph.D. degree in information and communication engineering from the Harbin Institute of Technology, Harbin, China, in 2011. He is currently a Professor with the Dalian University of Technology, China. He won the Best Paper Awards in IEEE VTC 2017 Spring, ICNC 2018, WCSP 2018, and WCSP 2019. He also received the IEEE Communications Society Asia Pacific Board Outstanding Young Researcher Award in 2018. He is serving on the Editorial Boards for IEEE WIRELESS COMMUNICATIONS and IEEE WIRELESS COMMUNICATIONS LETTERS.

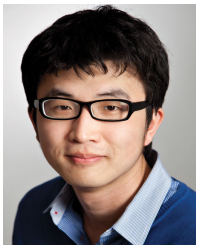

Zheng Chang (Senior Member, IEEE) received the Ph.D. degree from the University of Jyväskylä, Jyväskylä, Finland, in 2013. He has published over 140 papers in journals and conferences. His research interests include the IoT, cloud/edge computing, security and privacy, vehicular networks, and green communications. He received the Best Paper Awards from IEEE TCGCC and APCC in 2017 and has been awarded as the 2018 IEEE Best Young Research Professional for EMEA and the 2021 IEEE MMTC Outstanding Young Researcher. He serves as an Editor for IEEE WIRELESS COMMUNICATIONS LETTERS, *Wireless Networks* (Springer), and *International Journal of Distributed Sensor Networks*, and a Guest Editor for *IEEE Network*, IEEE WIRELESS COMMUNICATIONS, *IEEE Communications Magazine*, IEEE INTERNET OF THINGS JOURNAL, IEEE TRANSACTIONS ON INDUSTRIAL INFORMATICS, *Physical Communications*, *EURASIP Journal on Wireless Communications and Networking*, and *Wireless Communications and Mobile Computing*. He was the Exemplary Reviewer of IEEE WIRELESS COMMUNICATION LETTERS in 2018. He has participated in organizing workshops and special sessions in GLOBECOM 2019, WCNC 2018–2022, SPAWC 2019, and ISWCS 2018. He also serves as the Symposium Co-Chair for IEEE ICC 2020 and IEEE GLOBECOM 2023, the Publicity Co-Chair for IEEE Infocom 2022, the Workshop Co-Chair for ICCC 2022, the TPC Co-Chair of IEEE iThing 2022, and a TPC Member for many IEEE major conferences, such as INFOCOM, ICC, and GLOBECOM.

Timo Hämäläinen (Senior Member, IEEE) has over 30 years of research and teaching experience in computer networks and networking security. He has led tens of external funded network management related projects. He has launched and led a Master's Program with the University of Jyväskylä (software and communications engineering) and teaches network management and security related courses. He has more than 220 internationally peer-reviewed publications and he has supervised over 40 Ph.D. theses. His research interests include network resource management, the IoT, and networking security.

Xianbin Wang (Fellow, IEEE) received the Ph.D. degree in electrical and computer engineering from the National University of Singapore in 2001.

He is currently a Professor and a Tier-1 Canada Research Chair with Western University, Canada. Prior to joining Western University, he was with the Communications Research Centre Canada as a Research Scientist/Senior Research Scientist from July 2002 to December 2007. From January 2001 to July 2002, he was a System Designer at STMicroelectronics. He has over 500 highly cited journals and conference papers, in addition to 30 granted and pending patents and several standard contributions. His current research interests include 5G/6G technologies, the Internet of Things, communications security, machine learning, and intelligent communications.

Dr. Wang is a fellow of the Canadian Academy of Engineering and a fellow of the Engineering Institute of Canada. He has received many prestigious awards and recognitions, including the IEEE Canada R. A. Fessenden Award, the Canada Research Chair, the Engineering Research Excellence Award at Western University, the Canadian Federal Government Public Service Award, the Ontario Early Researcher Award, and six IEEE best paper awards. He was involved in many IEEE conferences, including GLOBECOM, ICC, VTC, PIMRC, WCNC, CCECE, and CWIT, in different roles, such as the General Chair, the Symposium Chair, a Tutorial Instructor, the Track Chair, the Session Chair, the TPC Co-Chair, and a Keynote Speaker. He was the Chair of the IEEE ComSoc Signal Processing and Computing for Communications (SPCC) Technical Committee and is also serving as the Central Area Chair for IEEE Canada. He also serves/has served as the Editor-in-Chief, an Associate Editor-in-Chief, and an editor/associate editor for over ten journals. He has been nominated as an IEEE Distinguished Lecturer several times during the last ten years. He is an IEEE Distinguished Lecturer.